



Fig. 3. An image labeled “occupancy” (space 1 in Fig. 2) Fig. 4. An image labeled “vacancy” (space 1 in Fig. 2)

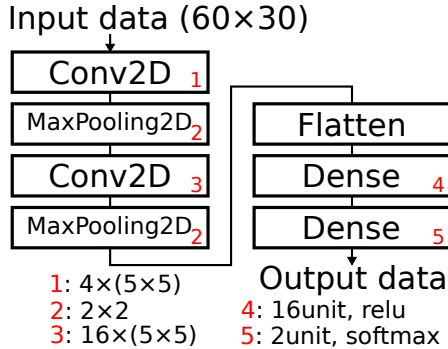


Fig. 5. Proposed CNN model

“vacancy.” Figs. 3 and 4 show extracted images with “occupancy” and “vacancy,” respectively. Each extracted image is resized to a resolution of 60×30, which is close to the size of space 1 in Fig. 2. Note that the parking space images resolution used in [6] is 224×224.

The CNN model implemented in this paper consists of seven layers in total, as shown in Fig. 5. We used Keras as the neural-network library for CNNs. Note that the CNN model parameters shown here were decided based on preliminary experimental results using various parameters including number of layers.

The first layer is a convolutional layer with four 5×5 filters, where features in the input image may be extracted. The second layer is a pooling layer whose size is 2×2. In this layer, the image size is reduced resulting in the calculation cost reduction while retaining the obtained features. In our model, two sets of the convolutional layer and the pooling layer are stacked. Therefore, the 1st to 4th layers consist of convolutional/pooling layers. On the 5th layer, a flatten layer, the values obtained by preceding four layers are smoothed and converted into one-dimensional data. In the 6th layer, a dense layer, the one-dimensional data is converted into 16 units using the ramp function. In 7th layer, again a dense layer and the final layer, the softmax function is used to convert the data with 16 units into two units, that is, “occupancy” or “vacancy.”

In this paper, the number of training/validation data is 79,029 including “occupancy” and “vacancy.” Among them, 3/4 is used for training and the remaining is used for validation. The batch size is 64 and the number of epochs is 20. As shown in Table I, the ratio of the number of training/validation and testing data is approximately (training/validation data):(testing data) = 4 : 1. Table II shows a summary of the car color ratio contained in the data labeled “occupancy.”

TABLE I
NUMBERS OF TRAINING, VALIDATION, AND TESTING DATA

	Number of	
	training/validation data	test data
Occupancy	40,207	10,000
Vacancy	38,822	10,000
Total	79,029	20,000

TABLE II
CAR COLOR BREAKDOWN IN LEARNING DATA

Color	Number of data	%
Black	16,168	40.2
Silver	12,244	30.5
White	6,560	16.3
Light blue	2,134	5.3
Red	1,602	4.0
Brown	1,499	3.7
Total	40,207	100.0

In this experiment, we acquired the parking space images with a webcam from the 11th floor of a building, where the parking spaces can be seen like Fig. 1. As the webcam, we used Logitech BRIO C1000eR with VGA resolution and 0.1 frame-per-second (fps). The data used in the experiment were obtained from 6:10 am to 4:30 pm.

III. COLOR-BASED PARKING DETECTION

As a comparison target of the proposed method, we investigate a color-based parking detection and its recognition rate. This color-based parking detection utilizes the RGB mode value for each parking space image. Here, the mode value is defined as the value which appears most frequently in a given image. In the case of “vacancy,” the mode value of each parking space image is expected to have a specific value, as we can see in Fig. 4. If the RGB mode value is in a specific value range, the space is judged as “vacancy.” Therefore, we need to find a typical mode value range for “vacancy” images. Note that the “vacancy” RGB mode value range is defined for each parking space. For each parking space i , the mean $(\mu_i^R, \mu_i^G, \mu_i^B)$ and the standard deviation $(\sigma_i^R, \sigma_i^G, \sigma_i^B)$ of the mode values for each RGB color component are calculated using the image labeled “vacancy.” The defined “vacancy” mode value range is given by

$$\begin{aligned}
 \mu_i^R - \alpha\sigma_i^R &\leq r_i \leq \mu_i^R + \alpha\sigma_i^R, \\
 \mu_i^G - \alpha\sigma_i^G &\leq g_i \leq \mu_i^G + \alpha\sigma_i^G, \\
 \mu_i^B - \alpha\sigma_i^B &\leq b_i \leq \mu_i^B + \alpha\sigma_i^B,
 \end{aligned} \tag{1}$$

where (r_i, g_i, b_i) is the RGB mode value of parking space i . The parameter α controls the range width. If α is 3, 99.7% of mode values of “vacancy” images for parking area i are expected within the defined range. If all three mode values, that is, (r_i, g_i, b_i) , are within the defined range, the system detects a given parking space i is “vacancy,” and otherwise “occupancy.”

TABLE III
RESULT OF THE PROPOSED CNN-BASED PARKING DETECTION
(NEAREST-NEIGHBOR INTERPOLATION)

		Proposed method		
		Occupancy	Vacancy	Accuracy
Ground truth	Occupancy	9,605	395	0.961
	Vacancy	371	9,629	0.963
F value		0.962		

TABLE IV
RESULT OF THE PROPOSED CNN-BASED PARKING DETECTION
(BILINEAR INTERPOLATION)

		Proposed method		
		Occupancy	Vacancy	Accuracy
Ground truth	Occupancy	9,600	400	0.960
	Vacancy	271	9,729	0.973
F value		0.966		

TABLE V
RESULT OF THE PROPOSED CNN-BASED PARKING DETECTION
(BICUBIC INTERPOLATION)

		Proposed method		
		Occupancy	Vacancy	Accuracy
Ground truth	Occupancy	9,990	10	0.999
	Vacancy	63	9,937	0.994
F value		0.996		

IV. EVALUATION

A. Proposed CNN-based parking detection

Since each parking space image is resized to a resolution of 60×30 , we used three interpolation methods, nearest neighbor, bilinear, and bicubic, whose results are shown in Tables III, IV, and V, respectively. As a result of testing using 10,000 images with the bicubic interpolation, the accuracy for both “occupancy” and “vacancy” was about 99%, resulting an F value of 0.996. In the following, we focus on the result of the bicubic interpolation.

Figs. 6 and 7 show the accuracy and the loss rate for each epoch, respectively, during training. The final accuracy and loss rate was about 0.99 and 0.003, respectively, for both the training and validation data.

To check the cause that “occupancy” detection is not 100%, we calculated the accuracy for each parking space and for each car color, which are shown in Tables VI and VII, respectively.

As for the accuracy dependency on the distance from the webcam and the parking space image resolution, from Fig. 1 and Table VI, we cannot see any clear correlations in this experiment. As for the accuracy dependency on the car colors, from Table VII, the accuracy for brown and black cars was not 100%. In the case of dark cars, it might be difficult to detect parking. Another possible reason the image acquisition environment. In this experiment, the webcam captures the lot images through a window of the building. Some captured images include undesired reflection since the window reflects light in some specific conditions.

Next, we discuss the result of testing data labeled “vacancy,” which is shown in the true negative (TN) column of Table VI. We found that the misjudged cases mostly occur in the

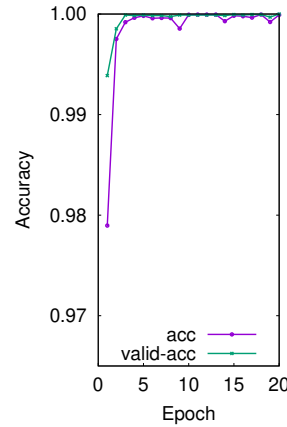


Fig. 6. Trajectory of the accuracy

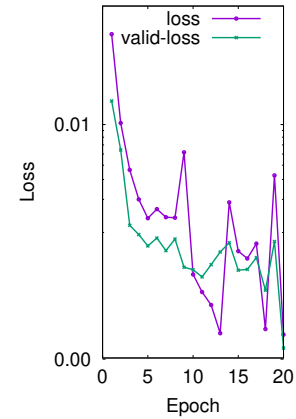


Fig. 7. Trajectory of the loss rate change

morning and evening images. In the morning, the shade and sunshine are clearly visible due to the sunlight, while, in the evening, the effect of the above mentioned window reflections becomes stronger.

B. Color-based parking detection

Table VIII shows the result by the color-based parking detection when $\alpha = 3$. The accuracy for “occupancy” was 23%, and the accuracy for “vacancy” was 99%, resulting an F value of 0.368. Since the parameter $\alpha = 3$ gives relatively large range for non-parking, the true positive (TR) rate, that is, the accuracy for “occupancy,” is relatively low. Fig. 8 shows the ROC curve plotted chaining the parameter α . Even from this figure, it can be seen that the performance is not good. The reason for the low accuracy is the difficulty to distinguish “vacancy” images and “occupancy” images by dark-colored cars, whose color is similar to the surface of the parking space in the “vacancy” images. Figs. 9 and 10 show histograms of the mode values for blue component with “vacancy” and “occupancy,” respectively, in the 18th parking space, where the accuracy was relatively low. The red dotted line is the threshold value, and the range between two red dotted lines is non-parking range. There is no significant difference in the shapes of the histograms for “vacancy” and “occupancy.” Therefore, the results might not become good even if we change the parameter α .

V. CONCLUSION

In this paper, we evaluated the proposed parking detection system using CNNs with commodity webcams. Also, we showed evaluation results of a color-based parking detection using the RGB mode values in parking space images as a comparison with the proposed approach. In the case of the proposed approach, the accuracy of “occupancy” was 99.9%, while that of “vacancy” was 99.4%. On the other hand, in the case of the color-based approach, the accuracy of “occupancy” was 22.6%, while that of “vacancy” was 99.1%. As for the color-based approach, it is difficult to determine whether

TABLE VI
ACCURACY FOR EACH PARKING SPACE

Parking space	TP rate %	TN rate %	Parking space	TP rate %	TN rate %
1	99	99	33	99	100
3	100	99	35	100	98
4	100	100	37	100	100
5	100	100	39	100	100
8	100	100	40	100	99
10	100	100	42	100	99
12	100	100	44	100	98
13	100	100	48	100	98
15	100	98	56	100	98
16	100	99	60	100	100
18	100	100	62	100	100
19	100	96	63	100	100
25	100	100	67	100	100
30	100	100	69	100	100
			82	100	98
Continued to the right column.			Total	99	99

TABLE VII
ACCURACY OF EACH CAR COLOR

	Number of		Accuracy (%)
	data	correct answers	
Red	391	391	100.0
Light blue	538	538	100.0
White	1,558	1,558	100.0
Silver	3,100	3,100	100.0
Brown	377	376	99.7
Black	4,036	4,027	99.8
Total	10,000	9,990	99.9

TABLE VIII
RESULT OF THE COLOR-BASED PARKING DETECTION ($\alpha = 3$)

		Color-based detection		
		Occupancy	Vacancy	Accuracy
Ground truth	Occupancy	2,257	7,743	0.226
	Vacancy	93	9,907	0.991
F value		0.368		

occupied or not according to the shown ROC curve. We found that it is possible to make a parking detection system with low-resolution cameras even at a relatively long distance.

ACKNOWLEDGMENTS

The authors would like to thank the GI-CoRE GSB, Hokkaido University for fruitful discussions. This work is supported in parts by the Ministry of Internal Affairs and Communications for SCOPE Program (185001003).

REFERENCES

[1] Z. Zhang, M. Tao, and H. Yuan, "A parking occupancy detection algorithm based on AMR sensor," *IEEE Sensors Journal*, vol. 15, no. 2, pp. 1261–1269, 2015.

[2] J. K. Suhr and H. G. Jung, "Sensor fusion-based vacant parking slot detection and tracking," *IEEE Transactions on Intelligent Transportation Systems*, vol. 15, no. 1, pp. 21–36, 2014.

[3] B. Guo and T. Damarla, "Improving acoustic vehicle classification by information fusion," *Pattern Anal. Appl.*, vol. 15, pp. 29–43, Feb. 2012.

[4] C. N. Dickson, A. M. Wallace, M. Kitchin, and B. Connor, "Improving infrared vehicle detection with polarisation," in *Proc. IET Intelligent Signal Processing Conference (ISP)*, 2013, pp. 1–6.

[5] J. Nyambal and R. Klein, "Automated parking space detection using convolutional neural networks," in *Proc. Pattern Recognition Association of South Africa and Robotics and Mechatronics International Conference (PRASA-RobMech)*, 2017, pp. 1–6.

[6] G. Amato, F. Carrara, F. Falchi, C. Gennaro, and C. Vairo, "Car parking occupancy detection using smart camera networks and deep learning," in *Proc. IEEE Symposium on Computers and Communication (ISCC)*, 2016, pp. 1212–1217.

[7] D. Poddar, S. Nagori, M. Mathew, D. Maji, and H. Garud, "Deep learning based parking spot detection and classification in fish-eye images," in *Proc. IEEE International Conference on Electronics, Computing and Communication Technologies (CONECCT)*, 2019, pp. 1–5.

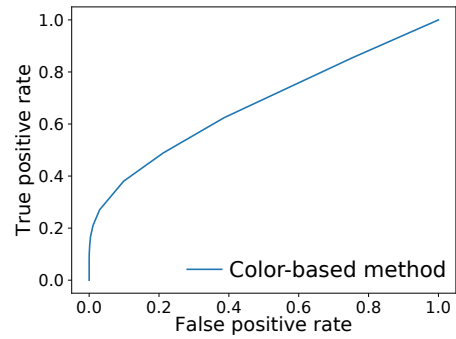


Fig. 8. ROC curve of the color-based approach

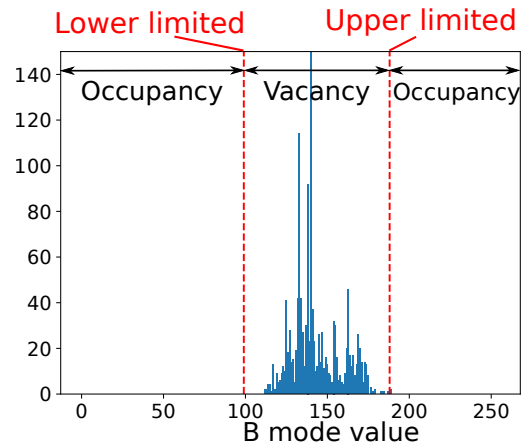


Fig. 9. Histogram of the mode values for blue component of the "vacancy" images

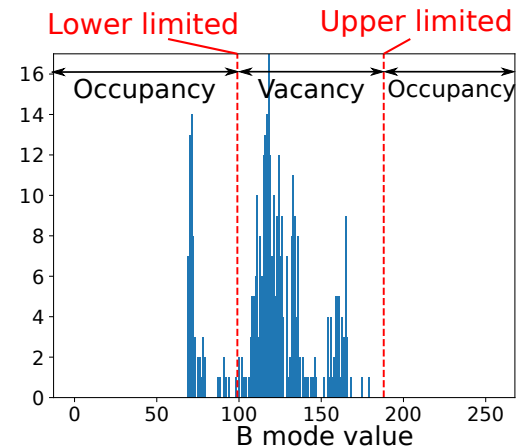


Fig. 10. Histogram of the mode values for blue component of the "occupancy" images